Available online at www.sciencedirect.com
ScienceDirect
International Journal of Heat and Mass Transfer 50 (2007) 897–901
International Journal of HEAT and MASS TRANSFER
www.elsevier.com/locate/ijhmt

Analytical solution for temperature profiles at the ends of thermal buffer tubes

Konstantin I. Matveev *, Gregory W. Swift, Scott Backhaus

Condensed Matter and Thermal Physics Group, Los Alamos National Laboratory, Los Alamos, NM 87545, United States

Received 1 May 2006; received in revised form 18 July 2006
Available online 9 October 2006

Abstract

The distortion of temperature profiles at the ends of thermal buffer tubes is related to the time-dependent gas pressure and motion in both nearly adiabatic and nearly isothermal environments during one acoustic cycle. The analytical solution for the mean temperature distribution is derived assuming zero heat conduction between gas parcels and linear acoustics with the acoustic wavelength much longer than other system dimensions. Theoretical results are compared with some experimental data and with results of numerical simulations that assume high heat conductivity.

Keywords: Thermoacoustics; Thermal buffer tube; Pulse tube; Interface; Transition

1. Introduction

A thermal buffer tube (TBT) or a pulse tube sometimes separates two heat exchangers (HX) kept at different temperatures (Fig. 1(a)) inside thermoacoustic systems [1]. The role of this tube is to pass acoustic power but to minimize heat transfer between the heat exchangers. The inevitable heat leak along the tube depends in part on thermal boundary conditions at the tube ends. These conditions are defined not only by the heat exchanger temperatures but also by the acoustic field.

The details of the temperature profile at the end of such a tube at the interface with a heat exchanger were described and calculated numerically by Smith and Romm [2,3] in the context of thermodynamic irreversibility. Subsequent theoretical or numerical results were presented by Bauwens [4–7], de Boer [8], Kittel [9,10], Swift [1], Weiland and Zinn [11], and Matveev et al. [12]. Storch et al. [13] and Matveev et al. [12] reported experimental results supporting the theoretical understanding. However, none of these publications presented an analytical solution for the time-averaged temperature as a function of position in the region of interest.

The goal of this study is to derive an approximate analytical solution for the mean temperature profile in the same framework, assuming linear acoustics and negligible heat conduction. Such a solution will provide faster estimation of this effect without conducting numerical simulations and will give further insights on thermal phenomena inside TBTs.

2. Problem description and assumptions

A one-dimensional schematic of the problem is shown in Fig. 1(b). The working gas is ideal. One-dimensional linear acoustic oscillations (along the x-axis) are present in the system. The acoustic wavelength is much longer than any distance in this part of the system. Twice the acoustic displacement is shorter than the tube length. Viscosity and wall effects are neglected. No mean flow is present. Under

* Corresponding author. Present address: MME School, Washington State University, Pullman, WA, 99164-2920, United States. Tel.: +1 509 335 1327; fax: +1 509 335 4662.
E-mail address: matveev@hydrofoils.org (K.I. Matveev).

0017-9310/$ - see front matter © 2006 Elsevier Ltd. All rights reserved.
doi:10.1016/j.ijheatmasstransfer.2006.08.004

Nomenclature

C	$\frac{\gamma-1}{\gamma}\frac{p_1}{p_m}$
p	pressure
T	Eulerian temperature
u	velocity
x	Eulerian coordinate
Y	defined by Eq. (12)

Greek symbols

φ	phase variable
γ	ratio of specific heats
θ	phase by which pressure oscillation leads velocity oscillation
Θ	Lagrangian temperature
ξ	Lagrangian coordinate
ψ	defined by Eq. (10)

Subscripts

HX	heat exchanger
m	mean
out	outside the doubled acoustic displacement
0	initial state
1	amplitude of sinusoidal motion
*	moment when gas parcel leaves heat exchanger

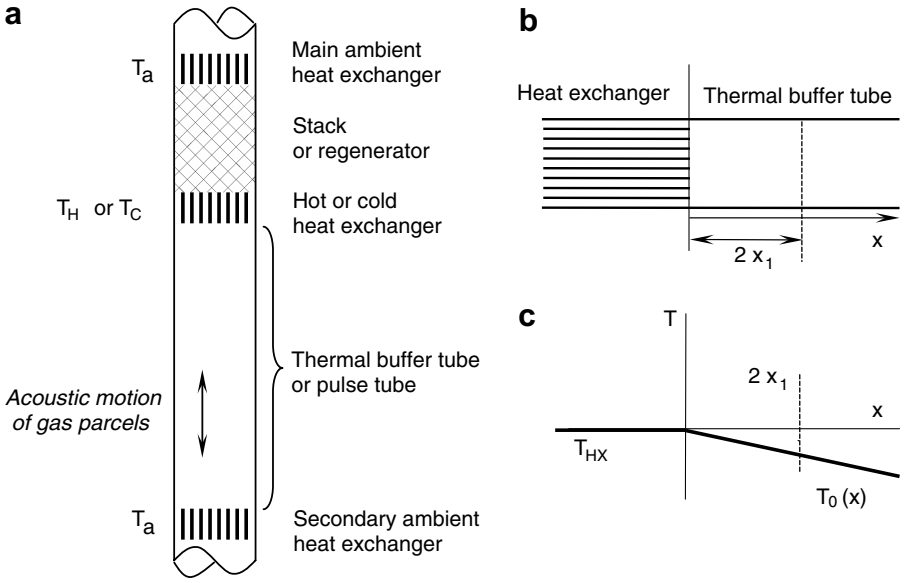

Fig. 1. (a) Typical part of a thermoacoustic system containing a thermal buffer tube or pulse tube. (b) Schematic drawing of the HX–TBT interface. (c) Example of a temperature profile at the beginning of an acoustic cycle.

these assumptions, a variation of the acoustic velocity amplitude, $\Delta u_1/u_1 \ll 1$, is small in the end zone $0 < x < 2x_1$, where $x = 0$ corresponds to the HX–TBT interface and x_1 is the acoustic displacement amplitude. This also implies relative smallness of the acoustic pressure amplitude, $2p_1/\gamma p_m \ll 1$. Therefore, all the gas parcels in the vicinity of the HX–TBT interface oscillate in phase, and the pressure fluctuation in the end zone is spatially uniform.

The environment is assumed isothermal inside the heat exchanger and nearly adiabatic inside the thermal buffer tube. A gas parcel entering the heat exchanger instantaneously acquires its temperature. A time-average linear temperature profile exists in the TBT beyond the doubled acoustic displacement, $2x_1$, from the HX–TBT interface. This temperature gradient implies a small but nonzero thermal conductivity of the gas. On the long time scale of many cycles, a small thermal conductivity can maintain a linear temperature profile for gas that never enters the heat exchanger, and on the time scale of one cycle such a small conductivity does not interfere with the evolving, continuous temperature profile of gas that has recently emerged from the heat exchanger. However, a small conductivity is not large enough to eliminate the temperature discontinuity at $x = 0$ that can occur when the gas reenters and strongly interacts with the isothermal heat exchanger.

Large temperature gradients are typically present in TBTs and pulse tubes. Cryogenic pulse tubes often span 200 K or more over a length of only 10 cm or less, with an average temperature of 200 K, with x_1 as large as 2 cm, and with $(\gamma-1)p_1/\gamma p_m \sim 0.06$. Thus, in the following analysis we will retain terms of order $\frac{\gamma-1}{\gamma}\frac{p_1}{p_m}\frac{x_1}{T_m}\frac{dT_{m,out}}{dx}$, while neglecting terms of order $\left(\frac{\gamma-1}{\gamma}\frac{p_1}{p_m}\right)^2$.

3. Analytical solution

The mean temperature profile inside the end zone, $0 < x < 2x_1$, can be found by averaging the temperature at each point of this zone over one acoustic cycle. We will track positions and temperatures of individual gas parcels in time, and then average temperatures at fixed points in space over an acoustic cycle. Instead of the time variable, we will use the phase variable φ, so the beginning of an acoustic cycle corresponds to $\varphi = 0$ and the end to $\varphi = 2\pi$.

The acoustic cycle is counted from the state when all gas parcels are in their leftmost positions. The phase-dependence of the gas-parcel coordinate ξ, velocity u, and total pressure p can be written as follows:

$$\xi(\varphi, \xi_0) = x_1(1 - \cos\varphi) + \xi_0, \tag{1}$$

$$u(\varphi) = u_1 \sin\varphi, \tag{2}$$

$$p(\varphi) = p_m + p_1 \sin(\varphi + \theta), \tag{3}$$

where ξ_0 is the initial position of a gas parcel, i.e., $\xi(0, \xi_0) = \xi_0$, p_m is the mean pressure, and θ is the phase shift between the acoustic pressure and velocity.

The initial, $\varphi = 0$ temperature distribution in the vicinity of the HX–TBT interface is the following (Fig. 1(c)):

$$T_0(x) = \begin{cases} T_{HX} & x < 0 \\ T_{HX} + x\frac{dT_{m,out}}{dx}(1 + C\sin\theta), & x > 0 \end{cases}, \tag{4}$$

where T_{HX} is the heat-exchanger temperature (constant), $\frac{dT_{m,out}}{dx}$ is the mean temperature gradient (constant) in the TBT outside $2x_1$, $C = \frac{\gamma-1}{\gamma}\frac{p_1}{p_m}$, and γ is the gas constant. The parcel inside the TBT that just touches the HX at the beginning of the acoustic cycle is assumed to have the HX temperature T_{HX}. The $C\sin\theta$ term in Eq. (4) is present to force the time averaged temperature gradient for $x > 2x_1$ to be equal to the assumed value $dT_{m,out}/dx$. The form of Eq. (4) ensures the continuity of the instantaneous temperature throughout the region $x > 0$, but it allows for a discontinuity at $x = 0$ while the gas is moving back into the HX.

The temperature variation of a gas parcel initially outside the heat exchanger, i.e., one with $\xi_0 > 0$, is

$$\Theta(\varphi, \xi_0) = T_0(\xi_0)\{1 + C[\sin(\varphi + \theta) - \sin\theta]\}. \tag{5}$$

For parcels initially inside the heat exchanger, i.e., those with $\xi_0 < 0$, this dependence is more complicated:

$$\Theta(\varphi, \xi_0) = \begin{cases} T_{HX}, & \xi(\varphi, \xi_0) < 0, \\ T_{HX}\{1 + C[\sin(\varphi + \theta) - \sin(\varphi_* + \theta)]\}, & \xi(\varphi, \xi_0) > 0, \end{cases} \tag{6}$$

where φ_* is the phase when such a gas parcel exits the heat exchanger in the first half of the acoustic cycle, which can be found from Eq. (1):

$$0 = x_1(1 - \cos\varphi_*) + \xi_0. \tag{7}$$

The mean temperature at any point in space is the average of the local temperature over a cycle:

$$T_m(x) = \frac{1}{2\pi}\int_0^{2\pi} T(\varphi, x)\,d\varphi, \tag{8}$$

where

$$T(\varphi, x) = \Theta(\varphi, x - x_1(1 - \cos\varphi)). \tag{9}$$

One can note that $\Theta(\varphi, \xi_0)$ and $T(\varphi, x)$ are, respectively, Lagrangian and Eulerian descriptions of temperature.

All information needed for calculating the integral in Eq. (8) is provided. At each point in $0 < x < 2x_1$, this integral can be represented as the sum of three integrals. The first integral covers the range $0 < \varphi < \psi(x)$, where

$$\psi(x) = \arccos\left(1 - \frac{x}{x_1}\right), \tag{10}$$

and involves the gas parcels traveling rightward through this point x in the first half of the cycle that were initially located between the heat exchanger and the given point. The second integral, covering the range $\psi(x) < \varphi < 2\pi - \psi(x)$, accounts for those parcels originating inside the heat exchanger that reach and pass through the point x twice during the cycle. The third integral accounts for the same parcels as in the first integral but on their way leftward during $2\pi - \psi(x) < \varphi < 2\pi$. Eq. (5) is used for Θ in the first and third integrals; Eq. (6) is used in the second. The result in the region $0 < x < 2x_1$ is

$$\begin{aligned} T_m(x) = {} & T_{HX} - \frac{x}{x_1}T_{HX}C\sin\theta \\ & - \frac{1}{\pi}\psi(x)\left[T_{HX}C\sin\theta + x_1\frac{dT_{m,out}}{dx}\left(1 - \frac{1}{2}C\sin\theta\right)\right] \\ & + \frac{1}{\pi}\frac{x}{x_1}\psi(x)\left(T_{HX}C\sin\theta + x_1\frac{dT_{m,out}}{dx}\right) \\ & + \frac{1}{\pi}\sin\psi(x)\left[T_{HX}C\sin\theta + x_1\frac{dT_{m,out}}{dx}(1 - C\sin\theta)\right] \\ & + \frac{1}{\pi}x\sin\psi(x)\frac{dT_{m,out}}{dx}C\sin\theta \\ & + \frac{1}{4\pi}\sin[2\psi(x)]x_1\frac{dT_{m,out}}{dx}C\sin\theta - \frac{1}{\pi}Y(x)T_{HX}C\cos\theta, \end{aligned} \tag{11}$$

where

$$Y(x) = \int_{\psi(x)}^{\pi}\sqrt{1 - \left(\frac{x}{x_1} + \cos\phi\right)^2}\,d\phi. \tag{12}$$

The function $Y(x)$ is monotonically decreasing from $Y(0) = 2$ to $Y(2x_1) = 0$. The approximation $Y \approx 2\left[1 - \left(\frac{x}{2x_1}\right)^{\pi/2}\right]$ is rather accurate and gives exact values for $Y(x)$ and its first derivatives at $x = 0$ and $x = 2x_1$.

From the obtained solution, the mean temperature at $2x_1$ and the mean temperature gradient beyond $2x_1$ inside TBT are related by

$$T_m(2x_1) = T_{HX}(1 - C\sin\theta) + x_1\frac{dT_{m,out}}{dx}\left(1 + \frac{1}{2}C\sin\theta\right). \tag{13}$$

If the second-order product $x_1 C$ is neglected, Eq. (13) is the same as Eq. (7.55) in Ref. [1]. The mean temperature at $2x_1$ and the temperature gradient beyond $2x_1$ are usually not known in advance (if only heat exchanger temperatures are given). Their values depend on various heat transfer mechanisms in TBT outside the end zone, such as heat conduction, heat convection by acoustic streaming, boundary-layer "entropy flow" [1], and so on. However, Eq. (13) establishes a relation between the temperature and its gradient at $2x_1$ for the outer region, which can serve as the thermal boundary condition for the heat transfer problem in the TBT outside the end zone.

4. Comparison with tests and enhanced-heat conductivity model

Temperature profiles given by Eq. (11) are compared with selected experimental data and results of numerical simulations that assumed a 100-fold augmented heat-conduction coefficient [12]. The reason for assuming an enhanced heat conductivity was the hypothesis of vorticity generation in the TBT end zone due to high-amplitude oscillating flow through the wire screens (flow straighteners) placed between the HX and the TBT in the tests. Comparisons of results are shown in Figs. 2 and 3 for four values of θ and for different temperature gradients in the TBT beyond $2x_1$. Steep temperature gradients in the figures correspond to gravitationally stable conditions, i.e., with the hot end of the TBT above its cold end. The working gas was helium at 3.45-bar mean pressure.

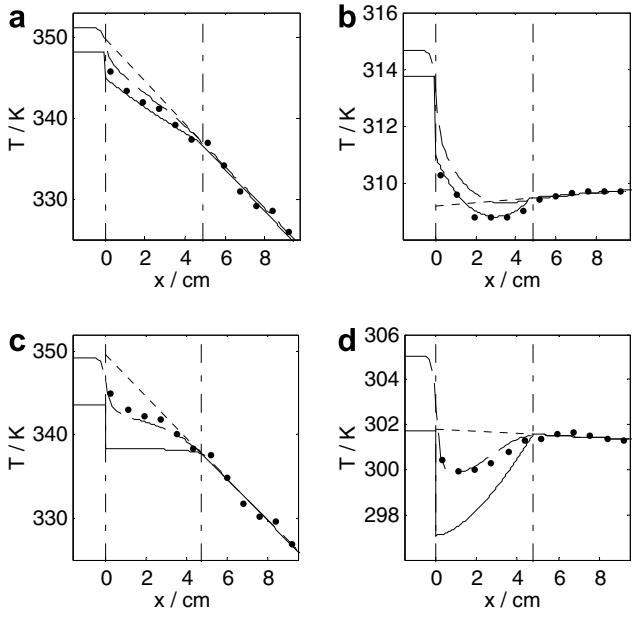

Fig. 2. Mean temperature profiles at the end of a TBT. (a) and (b) $p_1/p_m = 0.05$ and $\theta = 45°$; (c) and (d) $p_1/p_m = 0.06$ and $\theta = 0°$. Dash–dotted vertical lines indicate the heat exchanger interface (at $x = 0$) and the peak-to-peak displacement from the heat exchanger interface into the TBT (near $x = 4.75$ cm); circles, measurements of gas mean temperature [2]; dotted line, the linear temperature profile estimated by extrapolating the mean temperature from beyond the doubled acoustic displacement back to the heat exchanger interface; dashed line, numerical solution for mean temperature profile using 100 times boosted heat-conduction coefficient [2]; solid line, analytical solution presented in this paper.

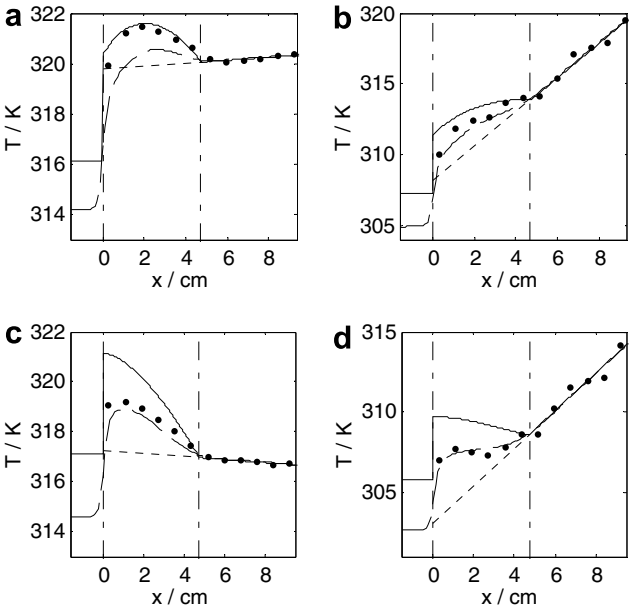

Fig. 3. Mean temperature profiles at the TBT end. (a) and (b) $p_1/p_m = 0.06$ and $\theta = -150°$; (c) and (d) $p_1/p_m = 0.05$ and $\theta = -180°$. All symbols are the same as in Fig. 2.

The theory presented in this paper demonstrates the correct sign of the temperature deviation at the TBT end zone from the linear temperature profile that exists at the absence of acoustic oscillations. The quantitative agreement between the theory and the experimental data is good at $\theta = 45°$ and $-150°$, but large overpredicting of the effect is observed at $\theta = 0°$ and $-180°$. The significant deviation of the slope of the theoretical temperature profile at the end zone from the slope of the temperature profile in the TBT outside the end zone is the most probable reason for this discrepancy. When this deviation is strong, i.e., at phases $0°$ and $-180°$, the heat conduction unaccounted by the theory starts to play a significant role, smoothing abrupt variations in the temperature slope. It was found that the molecular heat conduction cannot provide smoothness at the levels observed in the experiments [12], but augmented heat conductivity (assumed to be caused by vortices shed from the mesh screens at the HX–TBT interface) makes a prediction in better correlation with the experimental data.

Therefore, the model developed here can be used for quantitative estimations when the predicted temperature deviation from the temperature profile extrapolated linearly from $2x_1$ back to the HX–TBT interface is relatively small. For significantly pronounced changes in the temperature profile, some empirical corrections can possibly be applied to reduce strong temperature distortions. If a system with a heat exchanger comprising parallel and very thin plates and without mesh screens at the HX–TBT interface is considered (i.e., flow disturbances over linear acous-

tic oscillations are minimal), then the theory is expected to predict temperature profiles more accurately.

It should be noted that regimes investigated by Matveev et al. [12] did not include standing-wave phasing, because of restrictions in the experimental apparatus. Results obtained on the boundary of the achievable acoustic domain (e.g., −120°) demonstrated a disagreement between results of numerical calculations and tests, which was attributed to high uncertainties of the test data at the extreme setting of the system. Therefore, our understanding of the phenomena near standing-wave phasing is not yet validated.

5. Conclusions

An approximate analytical solution is presented for temperature profiles at the ends of thermal buffer tubes, assuming zero heat conduction. This solution correlates well with test results for a system with small-scale vorticity source when predicted temperature distortions are relatively small. Better agreement of this theory with tests is found at acoustic phases midway between standing and traveling waves.

Acknowledgement

This work was supported by OBES/DMS in the US Department of Energy's Office of Science.

References

[1] G.W. Swift, Thermoacoustics: A Unifying Perspective for Some Engines and Refrigerators, Acoustical Society of America, Sewickley, PA, 2002.

[2] J.L. Smith, M.J. Romm, Thermodynamic loss at component interfaces in Stirling cycles, in: Proceedings of the Twenty Seventh Intersociety Energy Conversion Engineering Conference, Society of Automotive Engineers, 1992, pp. 5.529–5.532.

[3] M.J. Romm, J.L. Smith, Stirling engine losses in dead volumes between components, in: Proceedings of the Twenty Eighth Intersociety Energy Conversion Engineering Conference, American Chemical Society, 1993, pp. 2.751–2.758.

[4] L. Bauwens, Adiabatic losses in Stirling cryocoolers: A stratified flow model, Cryogenics 34 (1994) 627–633.

[5] L. Bauwens, Adiabatic losses in Stirling refrigerators, Trans. ASME J. Energy Resour. Technol. 118 (1996) 120–127.

[6] L. Bauwens, Interface loss in the small amplitude orifice pulse tube model, in: P. Kittel (Ed.), Advances in Cryogenic Engineering, Vol. 43, Plenum Press, New York, 1998, pp. 1933–1940.

[7] L. Bauwens, Stirling cryocooler model with stratified cylinders and quasisteady heat exchanger, J. Thermophys. Heat Transfer 9 (1) (1998) 129–135.

[8] P.C.T. de Boer, Thermodynamic analysis of the basic pulse-tube refrigerator, Cryogenics 34 (1994) 699–711.

[9] P. Kittel, The temperature profile within pulse tubes, in: P. Kittel (Ed.), Advances in Cryogenic Engineering, Vol. 43, Plenum Press, New York, 1998, pp. 1927–1932.

[10] P. Kittel, Enthalpy, entropy, and exergy flow losses in pulse tube cryocoolers, in: R.G. Ross (Ed.), Cryocoolers, Vol. 13, Springer, 2005, pp. 343–352.

[11] N.T. Weiland, B.T. Zinn, Open cycle traveling wave thermoacoustics: Mean temperature difference at the regenerator interface, J. Acoust. Soc. Am. 114 (2003) 2791–2798.

[12] K.I. Matveev, G.W. Swift, S. Backhaus, Temperatures near the interface between an ideal heat exchanger and a thermal buffer tube or pulse tube, Int. J. Heat Mass Transfer 49 (2006) 868–878.

[13] P.J. Storch, R. Radebaugh and J.E. Zimmerman, Analytical model for the refrigeration power of the orifice pulse tube refrigerator, Technical note 1343, National Institute of Standards and Technology 1990.